Absolute Quantitation of Phosphopeptides and Glycopeptides Using Coulometric Mass Spectrometry (CMS)

Md. Tanim-Al Hassan[1], Yongling Ai[1], Bhavya Deshaboina[1], Timothy Yaroshuk[1], Arjun Sharma[1], Quentin Young[1], Howard D. Dewald[2] and Hao Chen[1,*]

[1]Department of Chemistry and Environmental Science, New Jersey Institutes of Technology, University Heights, Newark, NJ 07102, USA, Email: hao.chen.2@njit.edu

[2]Chemistry & Biochemistry Department, Ohio University, Athens, OH 45701, USA

Revised for *ACS Measurement Science Au*

Abstract

Phosphorylation and glycosylation are two important protein post-transitional modifications (PTMs). However, quantification of these PTMs is challenging due to the lack of protein or peptide standards. In this study we introduced a novel approach using coulometric mass spectrometry (CMS) for absolute quantitation of phosphopeptides and glycopeptides without using standards. First, phosphorylated tyrosine peptides such as TSTEPQpYQPGENL and RRLIEDAEpYAARG can be converted into electrochemically active tyrosine peptides via enzymatic phosphate removal using alkaline phosphatase, prior to CMS quantitation. Accurate quantitation was obtained with small quantitation errors (0.3-6.6%). Alternatively, for electrochemically inactive phosphopeptides and glycopeptides, derivatization of their N-termini with an NHS ester reagent, 2,5-dioxo-1-pyrrolidinyl 3,4-dihydroxybenzene propanoate (DPDP), was conducted to introduce one electroactive catechol tag, allowing the DPDP-derivatized peptides to be quantified by CMS. This strategy was first validated using peptides RGD, GGYR, phosphopeptide RRApSVA and glycopeptide NYIVGQPSS(β-GlcNAc)TGNL-OH and successful quantification was achieved with quantification errors less than 6%. Taking one step further, we applied this approach to quantify glycopeptides generated from tryptic digestion of NIST monoclonal antibody (mAb). Through HILIC column separation, five N297 glycopeptides were successfully derivatized, separated and quantified by CMS without the use of standards. Due to the biological significance of PTMs, this study for quantifying peptides carrying PTMs would have a high potential for quantitative proteomics and biological research.

Keywords: phosphopeptide; glycopeptide; post-translational modification; absolute quantitation; electrochemistry; mass spectrometry.

Introduction

Phosphorylation and glycosylation are among the most common and extensively studied post-translational modifications (PTMs).[1-7] About 30% of the human proteome is phosphorylated, and phosphoprotein may exist as multiple phosphorylated forms.[8] There are two main kinds of phosphorylation: O-phosphorylation, which occurs on serine, threonine, and tyrosine residues; and N-phosphorylation, which takes places on histidine, arginine, and lysine.[9] Glycosylation plays various roles in the structure and function of proteins, and alterations in lycosylation could lead to numerous diseases including cancer and immune system deficiencies.[10-12] N-glycosylation occurs mainly at asparagine (Asn or N) residues where the consensus tripeptide sequence NXS/T is located (where X is any amino acid except proline). At least one N-glycosylation motif is present in two-thirds of all human proteins, and ca. 50% of all human proteins are N-glycosylated. Other types of glycosylation include O-glycosylation, which occurs in the serine and threonine residues, and C-glycosylation which bonds on the indole rings of the tryptophan residues.[13, 14]

In proteomics research, quantitative information of peptides and proteins is critical for helping us to understand biological processes. Quantification in mass spectrometry (MS)-based proteomics research relies on two fundamental strategies: relative and absolute quantitation.[15-19] Relative quantitation methods involve comparing the levels of peptides or proteins among different samples.[20] Traditionally label-free approach involves analyzing samples and comparing their mass spectra to determine peptide abundances relative to another sample.[21, 22] Alternatively, isotopic labeling is commonly used in relative quantitation, where peptides from two samples are labeled with heavy and light isotopes.[23, 24] The intensities of these labeled peptides are then compared to discern changes in abundance between the samples.[23, 25-27] Elegant approaches like tandem mass tag (TMT), isotope-coded affinity tags (ICAT), stable isotope labeling by amino acids in cell

culture (SILAC), isobaric tags for relative and absolute quantitation (iTRAQ), metal element chelated tags (MECT), isotope-coded protein labeling (ICPL), and N, N-dimethyl leucine (DiLeu) isobaric tag methods fall under this category.[28-36] Likewise, absolute quantitation of proteins involves spiking a known quantity of isotope-labeled target peptide into an experimental sample, followed by LC-MS or LC-MS/MS analysis.[18, 21, 37-49] The three most well-known methods for absolute quantitation are absolute quantification (AQUA), quantification conCATamer (QconCAT) and protein standard absolute quantification (PSAQ).[17] While these elegant techniques offer the advantage of determining the absolute amounts of target peptides across different samples, the necessity for using standard or isotope-labeled peptides poses challenges. These standard peptides may not always be readily available, and their synthesis can be expensive and time-consuming.[18, 19, 22] Thus, the quest for a standard-free absolute quantitation method remains an ideal goal in the field of proteomics research. This is particularly true for quantifying protein PTMs such as phosphorylation and glycosylation in which the standard phosphopeptides or glycopeptides may be even more difficult to obtain.

Recently, we developed coulometric mass spectrometry (CMS) for absolute quantitation of electroactive analytes, using liquid chromatography/electrochemistry/mass spectrometry (LC/EC/MS) apparatus (illustrated in Figure S1).[15-19, 50-53] The method is based on electrochemical oxidation/reduction of analytes followed by MS to measure the oxidation/reduction yield. Electrochemical reaction results in an electric current response, which can be integrated over time to calculate the electric charge Q involved in the redox reaction. According to Faraday's Law, Q is proportional to quantity of the oxidized/reduced analyte: $Q = nzF$, where n is the moles of the oxidized/reduced analyte, z is the number of electrons transferred per molecule during the redox reaction, and F is the Faraday's constant (9.65×10^4 C/mol). Therefore, the moles of the

oxidized/reduced analyte can be calculated as $n = Q/zF$. Meanwhile, upon oxidation or reduction, the target analyte shows a reduced intensity in the acquired MS spectra, and the relative analyte ion intensity change Δi, reflects the redox conversion yield. Thus, the moles of the oxidized/reduced analyte, in combination with the conversion yield, can be used to calculate the total amount of the analyte. In other words,

Total amount of the analyte = (amount of the oxidized/reduced analyte)/(the conversion yield)

= (amount of the oxidized/reduced analyte)/(the conversion yield)

$= Q/(zF\Delta i)$ (eq. 1)

With this CMS method, we conducted absolute quantitation of peptides and proteins based on electrochemical oxidation of oxidizable cysteine, tyrosine and tryptophan residues.[15-19, 50-53] For peptides without oxidizable residues, they could be derivatized to carry an electrochemical tag such as methylene blue,[17] allowing them to be quantifiable by CMS after derivatization. In this study, we extended the CMS quantitation approach for peptides with PTMs such as phosphopeptides and glycopeptides. For phosphorylated tyrosine peptides, their phosphates were removed enzymatically to generate electroactive tyrosine peptides (Scheme 1a), before CMS quantitation. Alternatively, for electrochemically non-active phosphopeptides or glycopeptides, peptide derivatization with DPDP (Scheme 1b) was performed to introduce one electroactive catechol tag, prior to CMS quantitation. Upon electrochemical oxidation at a low oxidation potential (0.7 V vs. Ag/AgCl), the catechol tag tends to lose two protons and two electrons to form a quinone product (z=2, Scheme 1b), facilitating CMS quantitation. Using these strategies, several phosphopeptides, glycopeptides as well as glycopeptides from NIST mAb digest were successfully quantified, without using standards.

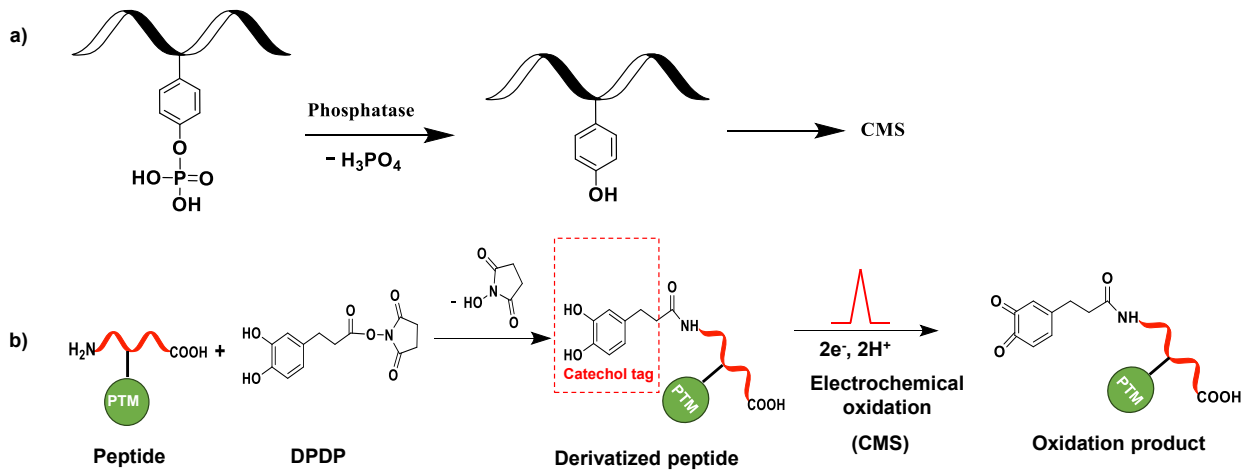

Scheme 1. Our approaches for absolute quantitation of a PTM-modified peptide by CMS a) after removing phosphate using phosphatase and b) after derivatization of its N-terminal with DPDP

Experimental Section

Chemicals

N-terminal protected amino acid BOC-Lys-OH, Gly-Gly-Tyr-Arg (GGYR, HPLC grade), Arg-Gly-Asp (RGD, HPLC grade), and 4-(2-hydroxyethyl)-1-piperazineethanesulfonic acid (HEPES) buffer were purchased from Sigma-Aldrich (St. Louis, MO). Phosphorylated RRApSVA (HPLC grade) was obtained from EMD Millipore (Temecula, CA). RRLIEDAEpYAARG, TSTEPQpYQPGENL, alkaline phosphatase (1 KU) from bovine intestinal mucosa and NIST mAb antibody were bought from Sigma-Aldrich (St. Louis, MO). NYIVGQPSS(*β*-GlcNAc)TGNL-OH was purchased from Sussex Research (ON, Canada). 2,5-Dioxo-1-pyrrolidinyl 3,4-dihydroxybenzene propanoate (DPDP) was bought from Aquila pharmatech LLC (Waterville, OH). Trypsin (sequencing grade) was purchased from Promega (Madison, WI). Dithiothreitol (DTT), iodoacetamide (IAA), ammonium bicarbonate (ABC) and sodium hydroxide were procured from Fisher Chemical (Fair Lawn, NJ). Formic acid (FA) and acetonitrile were

obtained from Fisher Chemical (Fair Lawn, NJ), and deionized water used for sample preparation was obtained using a Millipore purification system (Burlington, MA).

Instrument

Our CMS system (apparatus shown in Figure S1) consisted of liquid chromatography (LC), electrochemistry (EC) and mass spectrometry (MS). Basically, an ultraperformance liquid chromatography (UPLC, Waters, Milford, MA) was connected with an electrochemical thin-layer flow cell equipped with either glassy carbon electrode (GCD, 6 mm ID) or boron-doped diamond electrode (BDD, 8 mm ID) as the working electrode (WE). The flow cell was further coupled with a high-resolution Orbitrap Q Exactive mass spectrometer (Thermo Scientific, San Jose, CA). An Ag/AgCl (3 M NaCl) electrode (RE, catalog no. MW-2021) was employed as a reference electrode (RE), while the stainless-steel body of the cell functioned as the counter electrode (CE).

Separation of peptides was achieved using either an Agilent poroshell reversed-phase column (HPH−C18, 2.1 mm × 100 mm, 1.9 μm, Agilent, Santa Clara, CA), reversed-phase column (BEH C18, 2.1 mm × 100 mm, 1.7 μm) or hydrophilic interaction liquid chromatography (HILIC) column (HALO Penta HILIC column, 2.1 mm × 250 mm; 2.7 μm, used for the separation of NIST mAb glycopeptides). The mobile phase flow rate was set at 0.2-0.3 mL/min. Mobile phase A used was water with 0.1 % FA and mobile phase B was acetonitrile with 0.1 % FA.

OriginPro 2018b was used to import and integrate the recorded electric current peak to calculate the total electric charge of Q. The peptide flowing out of electrochemical cell was online analyzed using the Orbitrap mass spectrometer equipped with a heated electrospray ionization (HESI) source with the following parameters: sheath gas flow rate, 35; auxiliary gas flow rate, 10; spray voltage, 3.0 kV; sweep gas flow rate, 0; capillary temperature, 300 °C; auxiliary gas heater temperature, 100 °C; S-lens RF level, 50. Mass spectra were acquired by Thermo Xcalibur

(3.0.63). Before each use, the glassy carbon working electrode underwent thorough cleaning by polishing with alumina slurry. *In situ* cleaning involved applying alternative positive and negative potentials of +2.0 V and -2.0 V was used for BDD electrode.

Cyclic voltammetry (CV) experiment

We first derivatized the GGYR peptide using DPDP and isolated the derivatized peptide, denoted as *GGYR (* represents the derivatized peptide) via fractionation by Shimadzu LC (LC 40B XR). Using a homemade undivided cell, we utilized 20 mL of 200 µM intact GGYR or 30 µM of *GGYR for the CV experiments conducted in a H_2O: ACN: FA (70:30:1). A 3 mm GCE electrode (GCE) with an area of 0.07 cm^2 served as the WE, while an Ag/AgCl reference electrode was positioned in close proximity to the WE to regulate the potential. Additionally, a carbon cloth of 5 cm^2 size was positioned opposite to the WE, serving as the CE. Monitoring and recording of the oxidation current were facilitated by an Epsilon EClipse™ potentiostat (BASi, West Lafayette, IN, USA).

Alkaline Phosphatase Treatment

Phosphatase was dissolved in 1 mL of 10 mM tris-HCL (pH 8.0) containing 1 mM magnesium chloride and then stored in fridge (4 ^oC). 50 µL of RRLIEDAEpYAARG (1 mM) or 100 µL of TSTEPQpYQPGENL (0.5 mM) was mixed with 20 µL alkaline phosphatase (0.86 KU/mL) respectively and incubated at 37°C for 1 h. Formic acid was added (final formic acid concentration: 1% by volume) after the dephosphorylation reaction. The sample was cooled to room temperature and diluted with 0.1% FA to final concentration of 1.0 µM for CMS analysis.

Protein digestion

A 40 µL of 10 µg/1µL (400 µg) of NIST mAb (Ref: 8671) was denatured using 80 µL of 8 M urea at room temperature and then vortexed for 15 min. 5 µL of 1 M DTT (freshly prepared) was added to the sample and then shaken for 1 h at 37 °C in a water bath. A 20 µL of 500 mM IAA was then added to the sample at room temperature in the dark for 30 min. The sample mixture was then desalted and buffer exchanged with 50 mM ABC buffer by Amicon 10K molecular weight cut-off filter (MWCOF) and then digested overnight with 20 µg trypsin (protein/trypsin ratio: 20:1).

Peptide derivatization with DPDP

For the proof-of-concept experiment, we first derivatized N-terminal protected amino acid BOC-Lys-OH with DPDP-NHS ester in 1:10 molar ratio using H_2O: ACN (50:50) as a solvent with pH 8.3 adjusted by NaOH. The sample was derivatized for overnight reaction using mild dark vortex. The same derivatization condition was applied for peptides RGD, RRA_pSVA and NYIVGQPSS(β-GlcNAc) TGNL-OH. To maintain a good buffering system for controlling pH and reduce reaction time, we also derivatized the GGYR peptide using 100 mM HEPES buffer (pH 8.3) and using a 1:10 molar ratio (peptide:DPDP) for the derivatization process.

For the derivatization of glycopeptides from mAb, the mAb digest sample was vacuum dried and reconstituted in 20 mM HEPES buffer (pH 8.5) to prepare a 5.3 µM sample, which was then shake with DPDP (159 mM, 3000-fold in excess) overnight in the dark for derivatization. The sample was dried out and reconstituted in ACN/H_2O (65:35 v/v) to prepare a 5.3 µM derivatized sample. An underivatized sample was also prepared to assist the measurement of the glycopeptide derivatization yields.

LC separation for CMS quantitation

For CMS quantitation of phosphopeptides RRLIEDAEpYAARG and TSTEPQpYQPGENL, after removal of phosphate, 10 µL of 1.0 µM peptide solution was injected by LC (10 pmol injection amount). The mobile phase flow rate was 200 µL/min. In a 10 min gradient elution mobile phase B increased from 2% to 70% in 3 min, and reached 90% in 1 min. Then, mobile phase B was kept at 90% for 3 min before returning to 2%.

For CMS quantitation of derivatized peptides, the LC elution program was similar, and the mobile phase flow rate was set 300 µL/min and 5 µL of 1 µM derivatized peptides (5 pmol injection amount) were injected for analysis. For the derivatized BOC-Lys-OH, LC gradient elution program started with 90 % A for 1 min, 90 % A to 40 % A in 8 min, linear gradient at 5 % A for 2 min and then 90% A for 2 min. For the derivatized RGD and phosphopeptide RRA_pSVA, LC gradient elution program started with 90 % A for 1 min, 90 % A to 80 % A in 3 min, linear gradient at 5 % A for 1 min and then 90 % A for 1 min. For the derivatized NYIVGQPSS(β-GlcNAc) TGNL-OH LC, gradient elution program started with 95 % A for 1 min, 95 % A to 70 % A in 10 min, linear gradient at 5 % A for 3 min and then 95 % A for 2 min. For the derivatized GGYR, the mobile phase started with 95 % A, 95 % A to 91 % A in 10 min, linear gradient at 5 % A for 2 min and then 95% A for 2 min. To avoid the interference of the HEPES buffer in the GGYR sample, the first 3 min of eluate was directed to waste.

For CMS quantitation of derivatized mAb glycopeptides, the mobile phase flow rate was set at 200 µL/ min. A gradient elution program starting with 25 % A for 5 min (the first 5 min of eluate was directed to waste), 25 % A to 35 % A in 30 min, linear gradient at 60 % A for 5 min and then 25% A for 5 min. A 10 µL of the derivatized mAb digest (5.3 µM, injection amount 53 pmol) was injected for CMS quantitation.

Results and Discussion

The integration of mass spectrometry (MS) with electrochemistry (EC), namely EC/MS, has drawn considerable attention and found many applications, including drug metabolism study, protein structural analysis, and electrochemical reaction mechanism elucidation.[54-59] The method can also be used to capture elusive reaction intermediates[60-69] and enable electrosynthetic reaction screening.[70-72] As a new application of the EC/MS technique, the unprecedented advantage of CMS is the capability of absolute quantitation without using any standards or establishing a calibration curve. In our previous research, we successfully demonstrated the capability of CMS to quantify peptides containing electroactive residues like cysteine, tyrosine and tryptophan.[15-19, 50-53] In this study, a similar CMS approach was adopted to quantify peptides containing phosphorylated tyrosine residues, after enzymatic removal of phosphate to generate electrochemically active tyrosine peptides. As the removal of phosphate by phosphatase is quantitative, the measured quantity of the resulting tyrosine peptide can reflect the amount of the phosphopeptide precursor. On the other hand, in a more general approach, phosphopeptides or glycopeptides can be selectively derivatized by DPDP to carry an electrochemical tag of catechol (Scheme 1b), prior to CMS quantitation. In comparison to our previously used methylene blue tag,[17] the catechol tag is more polar and water soluble, leading to better peptide separation by LC and therefore benefits CMS quantitation.

CMS quantitation of phosphopeptides after phosphate removal

To explore the feasibility of CMS quantitation of phosphorylated tyrosine peptides, one standard peptide TSTEPQpYQPGENL was first tested. As shown in Figure 1a and 1b, after incubation with alkaline phosphatase, the TSTEPQpYQPGENL was quantitatively[73-75] converted into TSTEPQYQPGENL (the original peak of TSTEPQpYQPGENL at 3.2 min disappeared (Figure 1a); instead, the product TSTEPQYQPGENL peak appeared at 3.5 min in the TIC diagram

(Figure 1b). When the intact TSTEPQpYQPGENL was injected, no electric current peak was observed with an applied of +1.05 V for oxidation (Figure 1g), indicating that phosphorylated tyrosine is not electrochemically active. In contrast, after the injection of the dephosphorylated

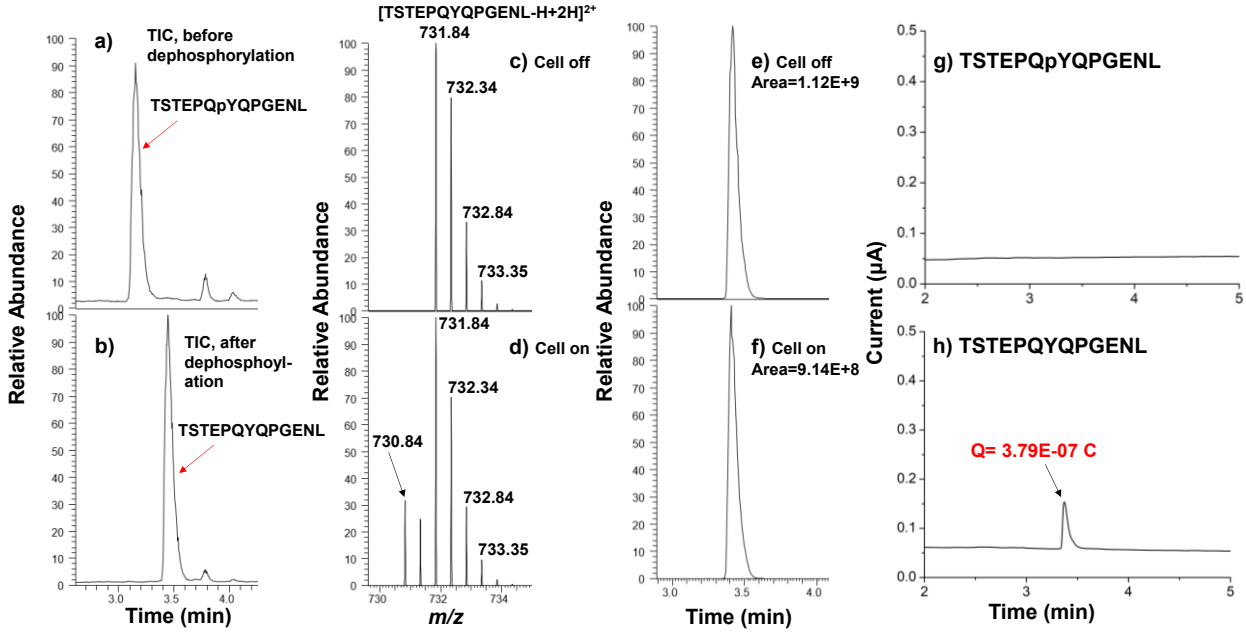

Figure 1. TICs of TSTEPQpYQPGENL a) before and b) after adding phosphatase. MS spectra of TSTEPQYQPGENL c) when the cell was off and (d) when the cell was turned on (applied potential: +1.05 V). The oxidation product of TSTEPQYQPGENL was detected at *m/z* 730.84. EICs of TSTEPQYQPGENL at *m/z* 731.84 were acquired e) when the cell was off and f) when the cell was turned on (applied potential: + 1.05 V). Electric current diagrams were collected from (g) TSTEPQpYQPGENL and (h) the oxidation of TSTEPQYQPGENL.

peptide TSTEPQYQPGENL sample, a sharp electric current peak was observed under the same oxidation conditions (Figure 1h), which is in line with our previous observation of electrochemical oxidation of tyrosine-containing peptides.[19, 53] Indeed, it was further confirmed by the corresponding MS spectra recorded upon electrochemical oxidation (Figures 1c and 1d). Compared to the MS spectrum (Figure 1c) without electrolysis, the +2 ion of TSTEPQYQPGENL was observed at *m/z* 731.84, whereas a new peak at *m/z* 730.84 (Figure 1d), corresponding to +2

ion of the oxidized peptide product and resulting from 2 electron and 2 proton losses upon tyrosine oxidation,[18, 19, 53] was detected, when +1.05 V was applied to the cell for oxidation. The integrated EIC peak area of *m/z* 730.84 shown in Figure 1f was reduced by 18.4% compared to the same peak in Figure 1e, suggesting that the oxidation yield for TSTEPQYQPGENL was 18.4% (see detailed data in Table S1). The amount of the oxidized TSTEPQYQPGENL was calculated to be 10.64 pmol, based on the integration of the current peak area shown in Figure 1h and the oxidation yield using eq. 1. Therefore, the measured amount of TSTEPQYQPGENL was 10.64 pmol (Table S1). A triplicate measurement gave the average amount of TSTEPQYQPGENL to be 10.66 pmol, which turned out to be close to the theoretical amount of 10.0 pmol, with the measurement error of 6.6% (Table S1).

RRLIEDAEpYAARG, another phosphopeptide that contains phosphotyrosine, was also analyzed in the same way by CMS. The RRLIEDAEpYAARG was also quantitatively converted into RRLIEDAEYAARG by phosphatase (Figure S2-a and S2-b). No electric current was detected for RRLIEDAEpYAARG (Figure S2-g), while a sharp current was observed for dephosphorylated peptide RRLIEDAEYAARG sample (Figure S2-h). The oxidation product was seen at *m/z* 506.27 after electrolysis (Figure S2-d). The oxidation yield was measured by the comparison of EIC peak area of *m/z* 506.94 before and after oxidation (Figures S2-e and S2-f). In a triplicate measurement, the averaged quantity of this peptide measured by CMS was 10.03 pmol which is very close to the initial amount of the expected value of 10.00 pmol with a measurement error 0.3% (detailed data is shown in Table S2). The results shown above confirm that CMS can be used for absolute quantitation of phosphorylated tyrosine peptides, in combination with enzymatic phosphate removal.

CMS quantitation after derivatization

Quantitation of standard amino acid and peptides

In this study, we also developed an alternative CMS approach for quantifying phosphopeptides and glycopeptides, in combination with DPDP derivatization strategy. First, we tested some model peptides to validate the quantitation method and then applied it to quantify phosphopeptides and glycopeptides.

We initially chose *N*-terminal protected amino acid BOC-Lys-OH as a model compound for our investigation. We observed a 94% reaction efficiency for this amino acid, as evidenced by a decrease in the EIC peak area of the intact peptide ion at *m/z* 247.1 from 5.80E6 before DPDP derivatization to 3.44E5 after DPDP derivatization (shown in Figure S3). For CMS quantitation, we injected 5 μL of 1 μM BOC-Lys-OH after its derivatization (injection amount: 5.0 pmol). Additionally, a minor potential of 0.7 V (vs. Ag/AgCl) was applied to the working electrode of the flow cell to facilitate the sample oxidation. Prior to oxidation, the +1 ion of DPDP-derivatized BOC-Lys-OH was detected at *m/z* 411.2 (Figure S4-a). Another peak at *m/z* 409.2 was also seen, probably due to in-source oxidation during sample ionization (Figure S4-a). Upon electrochemical oxidation, the intensity of the +1 ion of the DPDP-derivatized BOC-Lys-OH decreased (Figure S4-b). Conversely, the intensity peak at *m/z* 409.2 increased (Figure S4-b), due to electrochemical oxidation. The extracted ion chromatogram (EIC) peak area of the DPDP-derivatized BOC-Lys-OH at *m/z* 411.2 decreased by 21% following oxidation (Figure S4-d) compared to its pre-oxidation EIC peak (Figure S4-c), indicating an oxidation yield of 21% (Table S3). The total charge involved in peptide oxidation was determined to be 1.67E-07C through integration of the peptide oxidation current (Figure S4-f). According to eq. 1 and z = 2 for the oxidation of the catechol moiety, it was determined that the amount of BOC-Lys-OH by CMS was 4.4 pmol, after considering 94% derivatization yield. In triplicate measurements, the average value of the three

runs was calculated to be 4.7 pmol (Table S3). The theoretical amount of BOC-Lys-OH used for CMS quantification was 5.0 pmol. The quantitation error of BOC-Lys-OH was -5.4% (Table S3), suggesting the quantitation feasibility of this alternative CMS approach.

Peptide RGD was then chosen as an additional test sample for CMS quantification method validation. A derivatization yield of 94% for this peptide using DPDP was measured using LC/MS in the similar way as described above for sample BOC-Lys-OH. Figure S5-a displays the +1 ion of the derivatized RGD (*m/z* 511.2) and its oxidized product (*m/z* 509.2, probably due to in-source oxidation). The EIC peak area of *m/z* 511.2 decreased by 10% following oxidation, indicating an oxidation yield of 10% (Figures S5c and S5d). The total charge Q during oxidation was recorded at 7.16E-8C. A theoretical 5.0 pmol of the peptide was injected, with an actual measured amount of 4.7 pmol (calculated based on eq. 1 with further consideration of the 94% derivatization yield, see details in Table S4), reflecting a slight measurement error of -6%.

Another peptide GGRY was also selected and derivatized by DPDP for test, for the reason to show that the catechol tag can be selectively oxidized without oxidizing its tyrosine residue when the applied potential is low. In order to gain deeper insights into the oxidation properties of DPDP derivatized peptide, we conducted cyclic voltammetry (CV) of intact GGYR and the derivatized GGRY, *GGYR. *GGRY was obtained by the reaction of GGYR with DPDP followed by LC purification. A 20 mL of 200 μM intact GGYR peptide (dissolved in H_2O: ACN: FA, 70:30:1 by volume) was conducted for CV. Upon initiating the CV experiment with a positive scan from 0 mV to 1400 mV (vs. Ag/AgCl), a discernible peak (I) at a potential of 1050 mV corresponding to the oxidization of the tyrosine residue of GGYR was observed as shown in Figure 2a (the observed onset oxidation potential for tyrosine is 900 mV). The oxidation of tyrosine at 1050 mV is consistent with our previous observation.[19] In contrast, when CV of 20 mL of 30 μM *GGYR

(dissolved in H_2O: ACN: FA, 70:30:1 by volume) was performed, two peaks (I & II) were noticed, corresponding to the oxidation of tyrosine moiety of *GGYR at 1050 mV (peak I, Figure 2b) and the oxidation of the catechol tag of *GGYR at 700 mV (the observed onset oxidation potential for the catechol tag is 620 mV, peak II, Figure 2b), respectively. A background CV in H_2O: ACN: FA (70:30:1 by volume) marked by

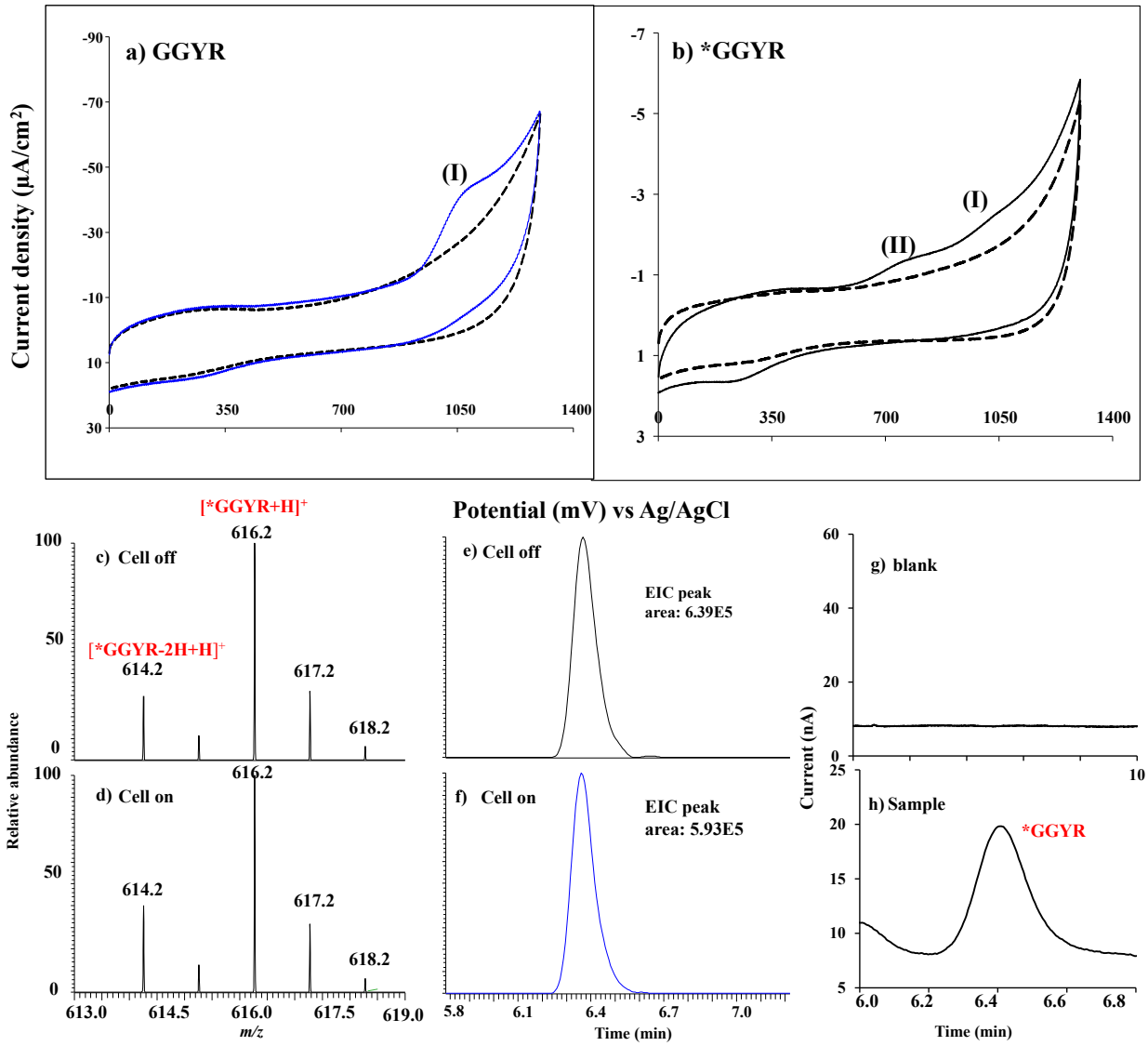

Figure 2. Cyclic voltammetric behaviors of a) GGYR and b) derivatized GGYR. Mass spectra of derivatized GGYR c) before electrochemical oxidation and d) after electrochemical oxidation at 0.7 V; EIC peaks of derivatized GGYR at *m/z* 616.2 e) before oxidation and f) after oxidation; Diagram showing the electrochemical oxidation currents of g) blank solvent and h) the derivatized GGYR sample.

dash lines in Figure 2a and 2b was also collected to separate faradic current from its non-faradic counterpart. From the CV plots shown in Figure 2a and Figure 2b, it was clear that the selective oxidation of the tag of the derivatized peptide without oxidizing the tyrosine residue can be achieved at a potential range between 620 and 900 mV. Therefore, in our experiment, 700 mV or 800 mV was selected as the oxidation potential for our CMS experiments. As it can be seen that our newly employed derivatizing agent DPDP offers a distinct advantage by undergoing oxidation at a lower potential of 0.7 V vs Ag/AgCl during CMS quantitation. This characteristic shows that it is less susceptible to the phenomenon of surface fouling on the electrode. Throughout our experimental endeavors, we observed a reduction in the frequency of electrode cleaning procedures.

In order to improve the efficiency of peptide derivatization using the DPDP reagent, 100 mM HEPES buffer (pH 8.3) was used as the buffer for GGYR derivatization and a 100% derivatization yield was achieved (no intact GGYR was seen after derivatization for 4 h), thus avoiding the necessity of measuring the derivatization yield. This process also significantly shortened the reaction time compared to the traditional overnight protocol. Subsequently, *GGRY was subject to CMS measurement. Before introducing the sample to the electrochemical cell, the first 3 minutes were diverted to waste to eliminate the HEPES buffer. When the cell was turned off, an ion of *m/z* 616.2 was observed (Figure 2c), corresponding to the protonated *GGRY. Another ion at *m/z* 614.2 was also seen (Figure 2c), probably due to in-source oxidation. The integrated EIC peak area for *m/z* 616.2 decreased by 7.2% following oxidation (Figures 2e and 2f), indicating a peptide oxidation yield of 7.2%. The total oxidation charge (*Q*) was calculated as 6.92E-08 C (Figure 2h). We injected an expected 5.0 pmol of peptide, with an actual measured

amount of 4.7 pmol (triplicate measurements, Table S5), yielding a small measurement error of -5.4%.

To verify that the oxidation did occur to the catechol tag located in the N-terminal of the *GGRY peptide, both the oxidized peptide product ion (*m/z* 614.2) and the intact peptide ion (*m/z* 616.2) were subject to MS/MS analysis. For this analysis, the *GGYR sample was introduced into the electrochemical cell for oxidation at 0.7 V using a syringe pump. The oxidation product was collected for analysis by nano-electrospray ionization, resulting in the detection of the oxidized G'GYR ion (' indicates the oxidized catechol tag) at *m/z* 614.2. As depicted in Figure S6, upon collision induced dissociation (CID), *m/z* 614.2 produced a fragment ion b_2-*2H* (*m/z* 277.1), whereas the intact *GGYR ion (*m/z* 616.2) generated b_2 (*m/z* 279.1), which is in line with the occurrence of oxidation to the N-terminal catechol tag of *GGYR indeed.

Our method's quantitation sensitivity was also evaluated by investigating of CMS quantitation by injecting 6 µL of 15 nM *GGYR sample (total amount: 150 fmol *GGYR). The integrated EIC peak area for *m/z* 616.2 decreased by 9.5% following oxidation (Figures S7c and 7d), indicating a peptide oxidation yield of 9.5%. The total oxidation charge (*Q*) was calculated as 2.54E-09 C (Figure S7f). The actual measured amount of 146 fmol by CMS (triplicate measurements, Table S6), showed a small measurement error of -3.0% in comparison with the theoretical injection amount of 150 fmol.

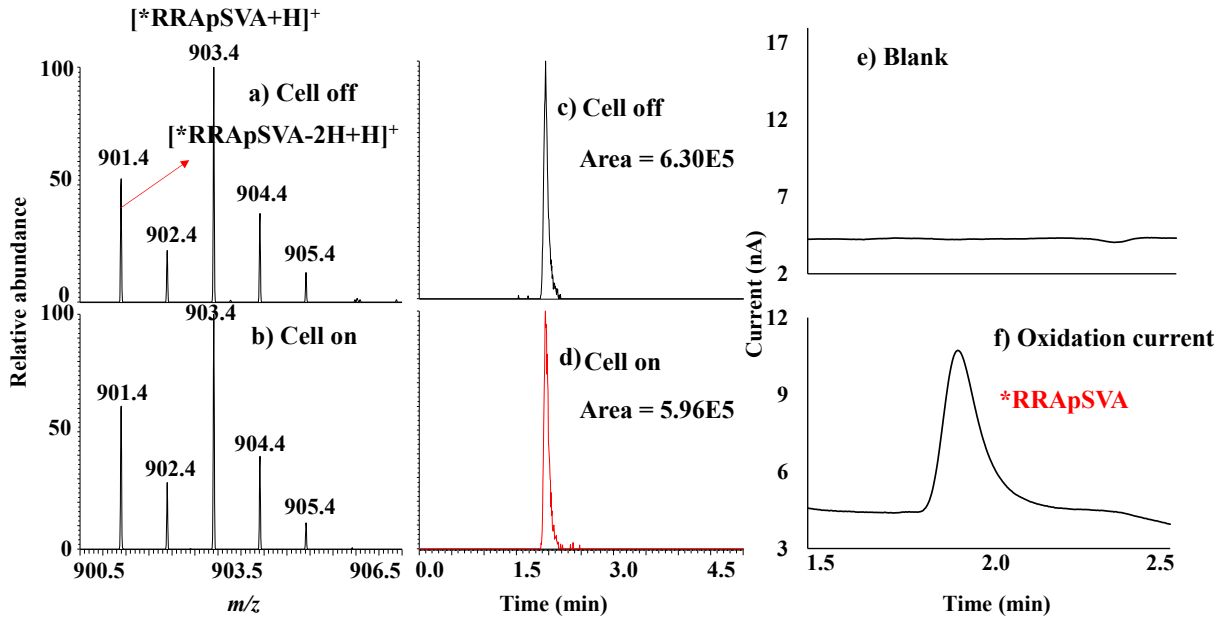

Figure 3. Mass spectra of the *RRApSVA a) before electrochemical oxidation and b) after electrochemical oxidation at 0.7V; EIC peaks of the *RRApSVA ion at *m/z* 904.4 c) before oxidation and d) after oxidation; Diagrams showing the electrochemical oxidation currents of e) blank solvent and f) *RRApSVA.

Quantification of phosphopeptides/glycopeptides

After quantifying standard peptides, we applied the method to quantify phosphopeptides and glycopeptides, as demonstration of its application. A phosphorylated peptide, RRApSVA, was selected as a test sample that has no oxidizable amino acid residue. The derivatization yield of this peptide was determined to be 68% by comparing the EIC peak area of the intact peptide (*m/z* 739.4) signal before and after the derivatization reaction (Table S7). Prior to oxidation, the +1 ion of derivatized RRApSVA was detected at *m/z* 903.4 (Figure 3a). An in-source oxidation peak was seen at *m/z* 901.4 (Figure 3a) and its signal intensity increased after triggering the oxidation by applying 0.7 V (vs. Ag/AgCl) to the WE of the cell (Figure 3b). In-source oxidation caused the measurement complexity due to an overlap of *m/z* 903.4 with the M+2 isotope peak of *m/z* 901.4. To avoid this complexity, we selected the peak of *m/z* 904.4 to calculate the oxidation yield. Upon

oxidation, the integrated EIC peak area for *m/z* 904.4 was reduced by 5.5% after oxidation (Figure 3d)

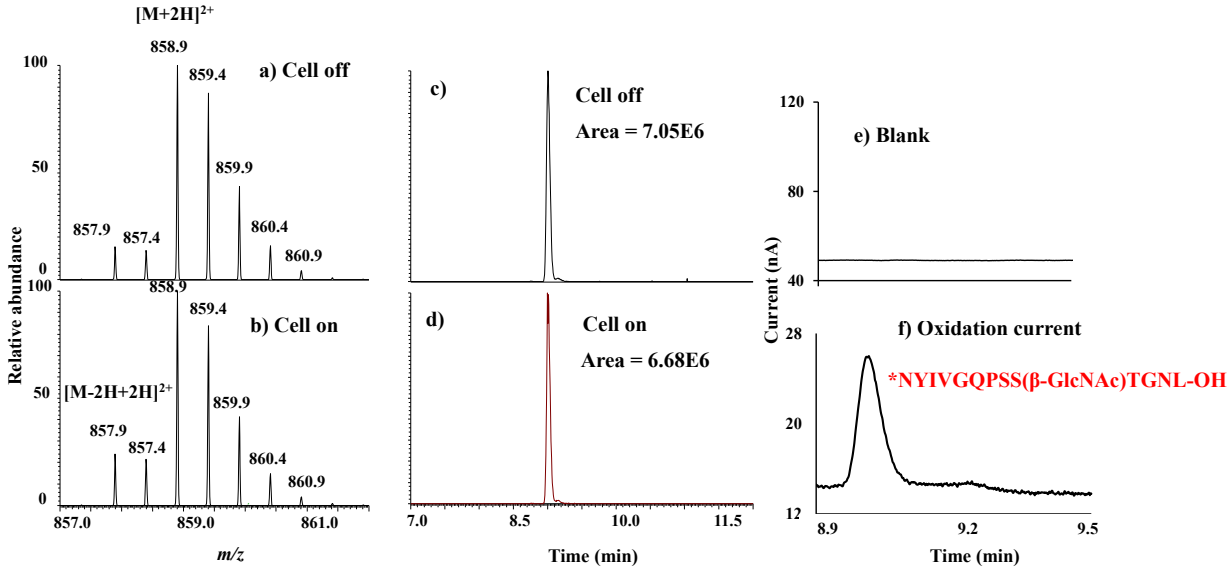

Figure 4. Mass spectra of the *NYIVGQPSS(β-GlcNAc)TGNL-OH a) before electrochemical oxidation at 0.7 V and b) after electrochemical oxidation; M represents *NYIVGQPSS(β-GlcNAc)TGNL-OH. EIC peaks of the *NYIVGQPSS(β-GlcNAc)TGNL-OH at *m/z* 859.9 c) before oxidation and d) after oxidation; Diagrams showing the electrochemical oxidation currents of e) blank solvent and f) *NYIVGQPSS(β-GlcNAc)TGNL-OH.

compared to before oxidation (Figure 3c), indicating the oxidation yield of 5.5%. The total charge *Q* involved in the oxidation in this case was determined to be 3.65E-08C (Figure 3f). This *Q* value, along with the oxidation yield (i.e., eq. 1), was utilized to calculate the quantity of the derivatized peptide to be 3.43 pmol (Table S7). Considering the 68% derivatization yield, the total peptide amount was calculated to be 5.0 pmol. Triplicate measurements gave an averaged peptide amount of 5.2 pmol (Table S7). Once again, this value aligns well with the theoretical peptide amount of 5 pmol, with a small quantitation error of 3.4% (Table S7).

To investigate the CMS quantification method for glycopeptide analysis, A glycosylated peptide, NYIVGQPSS(β-GlcNAc)TGNL-OH, was selected for testing. The derivatization yield of

this peptide was determined to be 98% by comparing the EIC peak area of the intact peptide (*m/z* 776.9) signal before and after the derivatization reaction (Table S8). The derivatized peptide was then measured using CMS. Before oxidation, the +1 ion of *NYIVGQPSS(β-GlcNAc)TGNL-OH was detected at *m/z* 858.9 (Figure 4a) and its isotope peak at *m/z* 859.9 was used for calculation of the oxidation yield. Upon peptide oxidation, the intensity at *m/z* 859.9 decreased by 5.3% after oxidation (Figure 4d) compared to no oxidation (Figure 4c), indicating the peptide oxidation yield of 5.3%. The total charge *Q* involved in the oxidation in this case was determined to be 5.2E-08C (Figure 4f). This *Q* value, along with the oxidation yield, was utilized to calculate the quantity of the derivatized peptide to be 5.13 pmol. Considering the 98% derivatization yield, the total averaged peptide amount was calculated to be 5.25 pmol (Table S8). Once again, this value aligns well with the theoretical peptide amount of 5 pmol, with a small quantitation error of 5.0%.

As shown above, several peptides including phosphopeptides and glycopeptides were tested in this study and the quantitation errors were good and within ±7%. The results are summarized in Table 1. The results suggest the feasibility and accuracy of our CMS for quantitation.

Table 1. Summary of CMS quantitation results for the measured peptides

Peptides	Injected amount (pmol)	Measured amount (pmol)	Quantification error (%)
BOC-Lys-OH	5	4.73	-5.4
RGD	5	4.70	-6.0
GGYR	5	4.73	-5.4
TSTEPQpYQPGENL	10	10.66	6.6
RRLIEDAEpYAARG	10	10.03	0.3
RRA_pSVA	5	5.20	3.4
NYIVGQPSS(β-GlcNAc) TGNL-OH	5	5.25	5.0

Quantitation of glycopeptides from IgG

As a demonstration of the application of our CMS approach, we applied it for quantifying glycopeptides of antibody IgG. MS techniques for antibody quantification in biotherapeutics typically employ a "bottom-up" strategy, in which proteins are enzymatically digested into peptides. However, quantitation of *N*-glycosylation is a challenging task. The lack of commercially available *N*-glycosylated standards precludes absolute quantitation, and thus, relative quantitation of glycosylation is performed by multiple reaction monitoring (MRM) method where relative comparisons of glycan/glycopeptide signals are taken into account.[76] In our study, using CMS after peptide derivatization, we enabled standard-free quantification of several glycopeptides originating from the heavy chain Fc of the IgG (located on the residue N297, see the sequence information of NIST monoclonal antibody (mAb) in SI). A

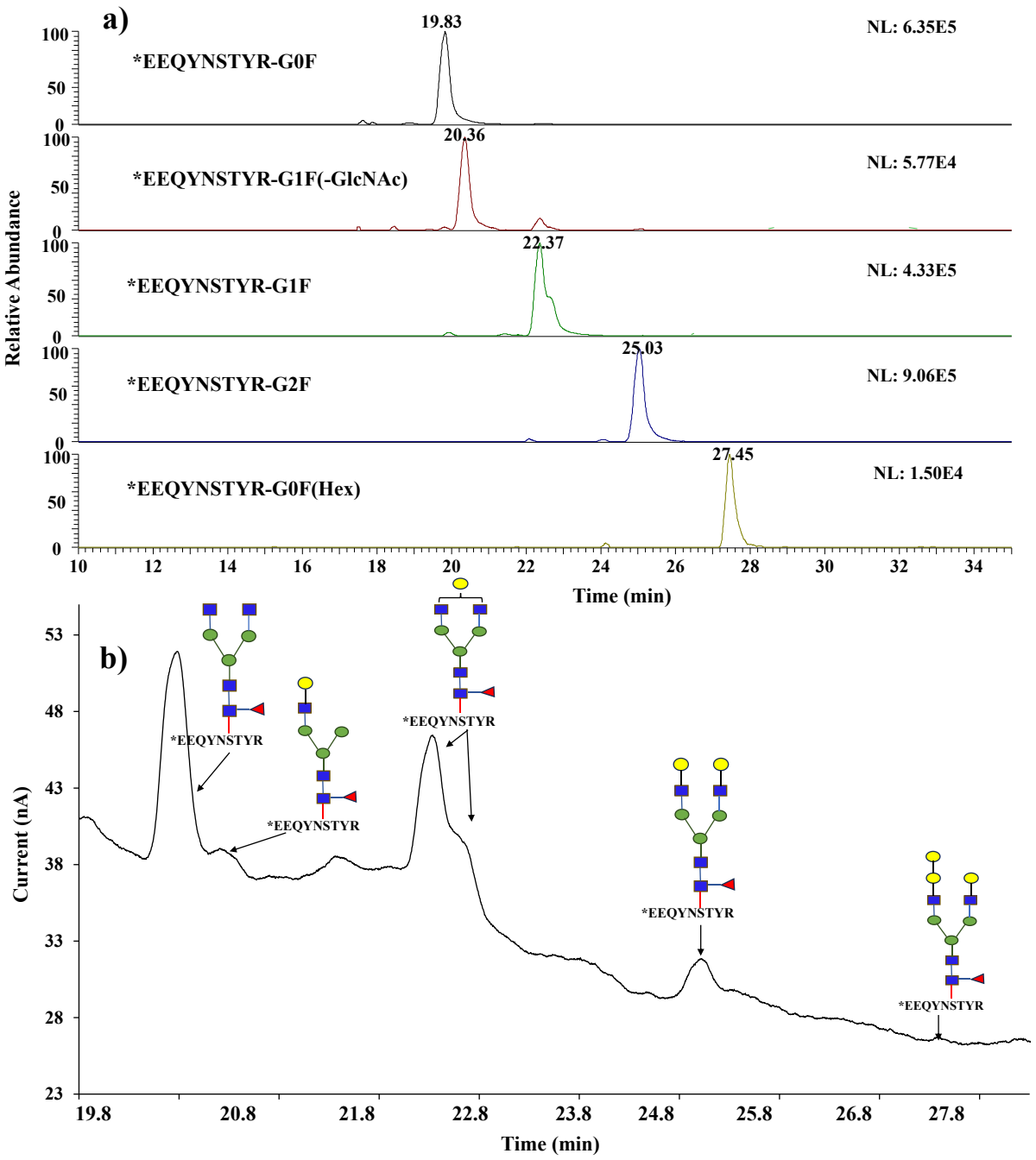

Figure 5. a) EICs of +2 ions of 5 glycopeptides from tryptic digestion of IgG after derivatization. b) electric current responses of the derivatized glycopeptides from IgG digest upon electrochemical oxidation.

HILIC column was used for the separation of these glycopeptides due to the high affinity of the glycopeptides.[77] Previously we reported NIST mAb glycopeptide quantitation by CMS but the direct electrochemical oxidation of those glycopeptides was complicated, due to the presence of two oxidizable tyrosine residues in them.[53] As the oxidation of one or both of the tyrosine residues occurred, the CMS quantitation required the assumption that the oxidation product resulting from one tyrosine oxidation has the same ionization efficiency as the oxidation product resulting from oxidation of two tyrosine residues, making the calculation not straightforward. In this study, we took the protocol to derivatize these glycopeptides with DPDP, so the oxidation at a low oxidation potential of 0.8 V could selectively occur to the catechol tags of the derivatized glycopeptides rather than the tyrosine residues, thus simplifying the quantitation calculation.

In our study, the NIST mAb was subjected to trypsin digestion, from which five glycopeptides (each with glycosylation at the N297 residue of the Fc heavy chain), EEQYNSTYR-G0F, EEQYNSTYR-G1F, EEQYNSTYR-G2F, EEQYNSTYR-G1F(-GlcNAc), and EEQYNSTYR-G2F(Hex) (structures shown in Table 2) were identified. The glycopeptides were derivatized using DPDP, and the derivatization yields were found to be 93-98% (Table S8). Subsequently, the derivatized glycopeptides were separated by a HILIC column and their EICs are shown in Figure 5a. The major glycoforms detected were *EEQYNSTYR-G0F, *EEQYNSTYR-G1F, and *EEQYNSTYR-G2F based on observed EIC peak intensities, while minor glycoforms included *EEQYNSTYR-G1F(-GlcNAc) and *EEQYNSTYR-G2F(Hex). It is noteworthy that *EEQYNSTYR-G1F exhibited a split peak at 22.4 min (the 3rd panel of Figure 5a) due to partial separation of glycan isomers resulting from differences in galactose α-3/6 linkage.[77] Additionally, the glycopeptide *EEQYNSTYR-G1F(-GlcNAc) eluted at 20.4 min (the second panel of Figure 5a), with an extra peak observed at 22.4 min most likely due to in-source fragmentation of the

*EEQYNSTYR-G1F ion. The electric oxidation current peaks of these derivatized glycopeptides are shown in Figure 5b.

Table 2. NIST mAb glycopeptides quantities measured by CMS

Glycopeptides	Glycan structures[a]	*m/z* of +2 ions of derivatized glycopeptides	RT (min)	Quantity measured by CMS (pmol)	Quantity measured by CMS (%)	Quantity measured by Zhao.et al.,[79] (%)
*EEQYNSTYR-G0F	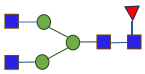	1399.55025	19.83	31.3	29.5	38.4
*EEQYNSTYR- G1F (-GlcNAc)	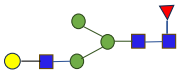	1379.03697	20.36	0.9	0.8	1.7
*EEQYNSTYR-G1F	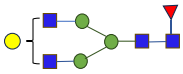	1480.57666	22.37	33.2	31.3	34.7
*EEQYNSTYR-G2F	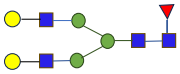	1561.60307	25.03	6.2	5.9	7.4
*EEQYNSTYR-G2F(Hex)	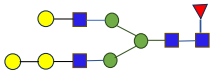	1642.62948	27.45	1.3	1.2	3.5
Total amount				72.9	68.7	85.7

[a]Structures using the Consortium for Functional Glycomics (CFG) Notation. Symbol representations of glycans: galactose = yellow circles, mannose = green circles, *N*acetylglucosamine = blues boxes, fucose = red triangles.

For CMS quantitation, prior to electrolysis, the doubly charged ion of *EEQYNSTYR-G0F was detected at *m/z* 1399.5 (Figure S8-a) along with in-source oxidation product peak at *m/z* 1398.5, whereas post-electrolysis analysis revealed the increased intensity of the oxidation product at *m/z* 1398.5 (Figure S8-b). To avoid interference of the isotope peak of the oxidized product to the ion intensity of the intact peptide ion, we chose the EIC area change from *m/z* 1401.0, the M +3

peak of *m/z* 1399.5, for the oxidation yield calculation. The oxidation yield for *EEQYNSTYR-G0F was determined to be 4.3% (Table S9) based on the EIC peak area drop of *m/z* 1401.0 upon oxidation (Figures S8-g and S8-h). The oxidation current was recorded 2.86E-7*C.* According to eq. 1, the measured amount of *EEQYNSTYR-G0F was 29.4 pmol (triplicate measurements, Table S9). Considering the 94% derivatization yield for this glycopeptide (Table S9), the amount of EEQYNSTYR-G0F was found to be 31.3 pmol. Similar calculations were performed for *EEQYNSTYR-G1F, *EEQYNSTYR-G2F, *EEQYNSTYR-G1F(-GlcNAc), and *EEQYNSTYR-G2F(Hex), yielding the measured quantities of 33.2, 6.2, 0.9, and 1.3 pmol, respectively (See Table S9, Figures S8 and S9). These glycopeptide quantities were also calculated relative to the theoretical total amount of IgG glycopeptides, which was 106 pmol (10 μL of 5.3 μM IgG, totaling 53.0 pmol which would produce 106 pmol glycopeptides in total by considering that one IgG has two symmetrical heavy chain totals), and listed in Table 2. The summative amount of the five measured glycopeptides was 72.9 pmol, which is in reasonable agreement with the theoretical value of 106 pmol, with a discrepancy of approximately -31.3% (Table 2). This discrepancy likely arose from sample losses during sample preparation such as enzymatic digestion or from the presence of additional minor glycopeptides that were not quantified.[78] Nevertheless, our CMS results thus provide an effective estimation of precursor glycoprotein quantity. Furthermore, our CMS results were compared with data from previous NIST mAb glycosylation studies by Zhao *et al*[79] which involved relative quantification of glycosylated peptides based on MS peak areas. As presented in Table 2, the relative abundances of the three major glycopeptides (*EEQYNSTYR-G0F, *EEQYNSTYR-G1F and*EEQYNSTYR-G2F) determined by CMS were close to the value reported by Zhao et al., representing (29.5% vs. 38.4%), (31.3% vs. 34.7%) and (5.9% vs. 7.4%) of total antibody abundance, respectively. While the relative

abundances determined by CMS and Zhao's method are similar, our CMS method uniquely provides absolute quantification for each glycopeptide. These findings underscore the effectiveness and potential utility of CMS for precise glycopeptide quantification.

Conclusions

In this study, we demonstrated an absolute quantitation strategy for quantifying phosphopeptides and glycopeptides by using the coulometric mass spectrometry approach in combination with an electrochemical labelling technique. Standard peptides, phosphopeptides and glycopeptides were successfully quantified by CMS with good quantitation accuracy. We also quantified glycopeptides from digested IgG. By this approach we were able to estimate the amount of glycoprotein based on the abundances of surrogate glycopeptides. The highlight of CMS is that it does not require an isotope-labeled standard to achieve absolute quantity, which has the potential to break the bottleneck in many current methods. It can be seen that our method could be also applicable for quantifying peptides or proteins with other types of PTMs such as *S*-nitrosation, *N*-acetylation, methylation, or lipidation, which could contribute to quantitative proteomics.

Acknowledgements

This work was supported by NSF (CHE-2203284), NIH (1R21GM148874-01) and New Jersey Health Foundation grants (PC 23-23 and PC 38-25).

Conflict of Interest

The authors declare no competing financial interest.

Author contributions

MTAH, YA, BD, TY, AS, and QY performed the investigation and performed the analysis. HC conceived the project idea and directed the research and HDD guided us on the electrochemistry experiments. MTAH, YA and HC wrote the manuscript.

Supporting Information

Additional CMS figures and data tables as well as experimental setup are included in Supporting information.

References

(1) Urban, J. A review on recent trends in the phosphoproteomics workflow. From sample preparation to data analysis. *Analytica Chimica Acta* **2022**, *1199*, 338857. DOI: https://doi.org/10.1016/j.aca.2021.338857.

(2) Zittlau, K.; Payal, N.; Claudia, C.-R.; Boris, M.; Philipp, S.; and Nalpas, N. Recent progress in quantitative phosphoproteomics. *Expert Review of Proteomics* **2023**, *20* (12), 469-482. DOI: 10.1080/14789450.2023.2295872.

(3) Cao, L.; Lih, T. M.; Hu, Y.; Schnaubelt, M.; Chen, S.-Y.; Zhou, Y.; Guo, C.; Dong, M.; Yang, W.; Eguez, R. V.; et al. Characterization of core fucosylation via sequential enzymatic treatments of intact glycopeptides and mass spectrometry analysis. *Nature Communications* **2022**, *13* (1), 3910. DOI: 10.1038/s41467-022-31472-4.

(4) Chen, S.-Y.; Clark, D. J.; Zhang, H. High-Throughput Analyses of Glycans, Glycosites, and Intact Glycopeptides Using C4-and C18/MAX-Tips and Liquid Handling System. *Current Protocols* **2021**, *1* (7), e186. DOI: https://doi.org/10.1002/cpz1.186 (acccessed 2025/04/03).

(5) Kawahara, R.; Chernykh, A.; Alagesan, K.; Bern, M.; Cao, W.; Chalkley, R. J.; Cheng, K.; Choo, M. S.; Edwards, N.; Goldman, R.; et al. Community evaluation of glycoproteomics informatics solutions reveals high-performance search strategies for serum glycopeptide analysis. *Nature Methods* **2021**, *18* (11), 1304-1316. DOI: 10.1038/s41592-021-01309-x.

(6) Yang, G.; Zhang, H.; Yi, W.; Yan, S.; Cao, L. Editorial: Protein Glycosylation—Advances in Identification, Characterization and Biological Function Elucidation Using Mass Spectrometry. *Frontiers in Chemistry* **2022**, *10*, Editorial. DOI: 10.3389/fchem.2022.847242.

(7) Xie, Y.; Liu, X.; Zhao, C.; Chen, S.; Wang, S.; Lin, Z.; Robison, F. M.; George, B. M.; Flynn, R. A.; Lebrilla, C. B.; et al. Development and application of GlycanDIA workflow for glycomic analysis. *bioRxiv* **2024**, 2024.2003.2012.584702. DOI: 10.1101/2024.03.12.584702.

(8) Seok, S.-H. Structural Insights into Protein Regulation by Phosphorylation and Substrate Recognition of Protein Kinases/Phosphatases. *Life* **2021**, *11* (9), 957. DOI: 10.3390/life11090957.

(9) Possemato, A. P.; Paulo, J. A.; Mulhern, D.; Guo, A.; Gygi, S. P.; Beausoleil, S. A. Multiplexed Phosphoproteomic Profiling Using Titanium Dioxide and Immunoaffinity Enrichments Reveals Complementary Phosphorylation Events. *Journal of proteome research* **2017**, *16* (4), 1506-1514. DOI: 10.1021/acs.jproteome.6b00905 PubMed.

(10) Imre, T.; Schlosser, G.; Pocsfalvi, G.; Siciliano, R.; Molnár-Szöllosi, E.; Kremmer, T.; Malorni, A.; Vékey, K. Glycosylation site analysis of human alpha-1-acid glycoprotein (AGP) by capillary liquid chromatography-electrospray mass spectrometry. *J Mass Spectrom* **2005**, *40* (11), 1472-1483. DOI: 10.1002/jms.938 From NLM.

(11) Banazadeh, A.; Veillon, L.; Wooding, K. M.; Zabet-moghaddam, M.; Mechref, Y. Recent advances in mass spectrometric analysis of glycoproteins. *ELECTROPHORESIS* **2017**, *38* (1), 162-189. DOI: https://doi.org/10.1002/elps.201600357 (acccessed 2025/04/03).

(12) Gutierrez-Reyes, C. D.; Jiang, P.; Atashi, M.; Bennett, A.; Yu, A.; Peng, W.; Zhong, J.; Mechref, Y. Advances in mass spectrometry-based glycoproteomics: An update covering the period 2017–2021. *ELECTROPHORESIS* **2022**, *43* (1-2), 370-387. DOI: https://doi.org/10.1002/elps.202100188 (acccessed 2025/04/03).

(13) Lee, J. Y.; Lee, H. K.; Park, G. W.; Hwang, H.; Jeong, H. K.; Yun, K. N.; Ji, E. S.; Kim, K. H.; Kim, J. S.; Kim, J. W.; et al. Characterization of Site-Specific N-Glycopeptide Isoforms of α-1-Acid Glycoprotein from an Interlaboratory Study Using LC–MS/MS. *Journal of Proteome Research* **2016**, *15* (12), 4146-4164. DOI: 10.1021/acs.jproteome.5b01159.

(14) Roberts, D. S.; Mann, M.; Melby, J. A.; Larson, E. J.; Zhu, Y.; Brasier, A. R.; Jin, S.; Ge, Y. Structural O-Glycoform Heterogeneity of the SARS-CoV-2 Spike Protein Receptor-Binding Domain Revealed by Top-Down Mass Spectrometry. *J Am Chem Soc* **2021**, *143* (31), 12014-12024. DOI: 10.1021/jacs.1c02713 From NLM.

(15) Ai, Y.; Gunawardena, H. P.; Li, X.; Kim, Y. I.; Dewald, H. D.; Chen, H. Standard-Free Absolute Quantitation of Antibody Deamidation Degradation and Host Cell Proteins by Coulometric Mass Spectrometry. *Anal Chem* **2022**, *94* (36), 12490-12499. DOI: 10.1021/acs.analchem.2c02709 From NLM.

(16) Ai, Y.; Zhao, P.; Fnu, P. I. J.; Chen, H. Absolute Quantitation of Tryptophan-Containing Peptides and Amyloid β-Peptide Fragments by Coulometric Mass Spectrometry. *J Am Soc Mass Spectrom* **2021**, *32* (7), 1771-1779. DOI: 10.1021/jasms.1c00121 From NLM.

(17) Fnu, P. I. J.; Tanim-Al-Hassan, M.; Yaroshuk, T.; Ai, Y.; Chen, H. Absolute Quantitation of Peptides and Proteins by Coulometric Mass Spectrometry After Derivatization. *Int J Mass Spectrom* **2024**, *495*. DOI: 10.1016/j.ijms.2023.117153 From NLM.

(18) Zhao, P.; Wang, Q.; Kaur, M.; Kim, Y.-I.; Dewald, H. D.; Mozziconacci, O.; Liu, Y.; Chen, H. Absolute Quantitation of Proteins by Coulometric Mass Spectrometry. *Analytical Chemistry* **2020**, *92* (11), 7877-7883. DOI: 10.1021/acs.analchem.0c01151.

(19) Zhao, P.; Zare, R. N.; Chen, H. Absolute Quantitation of Oxidizable Peptides by Coulometric Mass Spectrometry. *J Am Soc Mass Spectrom* **2019**, *30* (11), 2398-2407. DOI: 10.1007/s13361-019-02299-z From NLM.

(20) Hoofnagle, A. N. Quantitative Clinical Proteomics by Liquid Chromatography–Tandem Mass Spectrometry: Assessing the Platform. *Clinical Chemistry* **2010**, *56* (2), 161-164. DOI: 10.1373/clinchem.2009.134049 (acccessed 5/11/2024).

(21) Xie, F.; Liu, T.; Qian, W.-J.; Petyuk, V. A.; Smith, R. D. Liquid Chromatography-Mass Spectrometry-based Quantitative Proteomics*. *Journal of Biological Chemistry* **2011**, *286* (29), 25443-25449. DOI: https://doi.org/10.1074/jbc.R110.199703.

(22) Wasinger, V. C.; Zeng, M.; Yau, Y. Current Status and Advances in Quantitative Proteomic Mass Spectrometry. *International Journal of Proteomics* **2013**, *2013*, 180605. DOI: 10.1155/2013/180605.

(23) Sohn, C. H.; Lee, J. E.; Sweredoski, M. J.; Graham, R. L.; Smith, G. T.; Hess, S.; Czerwieniec, G.; Loo, J. A.; Deshaies, R. J.; Beauchamp, J. L. Click chemistry facilitates formation of reporter ions and simplified synthesis of amine-reactive multiplexed isobaric tags for protein quantification. *J Am Chem Soc* **2012**, *134* (5), 2672-2680. DOI: 10.1021/ja2099003 From NLM.

(24) Tan, H.; Wu, Z.; Wang, H.; Bai, B.; Li, Y.; Wang, X.; Zhai, B.; Beach, T. G.; Peng, J. Refined phosphopeptide enrichment by phosphate additive and the analysis of human brain phosphoproteome. *PROTEOMICS* **2015**, *15* (2-3), 500-507. DOI: https://doi.org/10.1002/pmic.201400171 (acccessed 2025/04/04).

(25) Gerber, S. A.; Rush, J.; Stemman, O.; Kirschner, M. W.; Gygi, S. P. Absolute quantification of proteins and phosphoproteins from cell lysates by tandem MS. *Proc Natl Acad Sci U S A* **2003**, *100* (12), 6940-6945. DOI: 10.1073/pnas.0832254100 From NLM.

(26) Calderón-Celis, F.; Diez-Fernández, S.; Costa-Fernández, J. M.; Encinar, J. R.; Calvete, J. J.; Sanz-Medel, A. Elemental Mass Spectrometry for Absolute Intact Protein Quantification without Protein-Specific Standards: Application to Snake Venomics. *Anal Chem* **2016**, *88* (19), 9699-9706. DOI: 10.1021/acs.analchem.6b02585 From NLM.

(27) Narumi, R.; Shimizu, Y.; Ukai-Tadenuma, M.; Ode, K. L.; Kanda, G. N.; Shinohara, Y.; Sato, A.; Matsumoto, K.; Ueda, H. R. Mass spectrometry-based absolute quantification reveals rhythmic variation of mouse circadian clock proteins. *Proc Natl Acad Sci U S A* **2016**, *113* (24), E3461-3467. DOI: 10.1073/pnas.1603799113 PubMed.

(28) Zhang, L.; Elias, J. E. Relative Protein Quantification Using Tandem Mass Tag Mass Spectrometry. In *Proteomics: Methods and Protocols*, Comai, L., Katz, J. E., Mallick, P. Eds.; Springer New York, 2017; pp 185-198.

(29) Colangelo, C. M.; Williams, K. R. Isotope-Coded Affinity Tags for Protein Quantification. In *New and Emerging Proteomic Techniques*, Nedelkov, D., Nelson, R. W. Eds.; Humana Press, 2006; pp 151-158.

(30) Ong, S.-E.; Blagoev, B.; Kratchmarova, I.; Kristensen, D. B.; Steen, H.; Pandey, A.; Mann, M. Stable Isotope Labeling by Amino Acids in Cell Culture, SILAC, as a Simple and Accurate Approach to Expression Proteomics*. *Molecular & Cellular Proteomics* **2002**, *1* (5), 376-386. DOI: https://doi.org/10.1074/mcp.M200025-MCP200.

(31) Vélez-Bermúdez, I. C.; Wen, T.-N.; Lan, P.; Schmidt, W. Isobaric Tag for Relative and Absolute Quantitation (iTRAQ)-Based Protein Profiling in Plants. In *Plant Proteostasis: Methods and Protocols*, Lois, L. M., Matthiesen, R. Eds.; Springer New York, 2016; pp 213-221.

(32) Liu, H.; Zhang, Y.; Wang, J.; Wang, D.; Zhou, C.; Cai, Y.; Qian, X. Method for Quantitative Proteomics Research by Using Metal Element Chelated Tags Coupled with Mass Spectrometry. *Analytical Chemistry* **2006**, *78* (18), 6614-6621. DOI: 10.1021/ac060895j.

(33) Chahrour, O.; Cobice, D.; Malone, J. Stable isotope labelling methods in mass spectrometry-based quantitative proteomics. *Journal of Pharmaceutical and Biomedical Analysis* **2015**, *113*, 2-20. DOI: https://doi.org/10.1016/j.jpba.2015.04.013.

(34) Xiang, F.; Ye, H.; Chen, R.; Fu, Q.; Li, L. N,N-dimethyl leucines as novel isobaric tandem mass tags for quantitative proteomics and peptidomics. *Anal Chem* **2010**, *82* (7), 2817-2825. DOI: 10.1021/ac902778d From NLM.

(35) Molden, R. C.; Goya, J.; Khan, Z.; Garcia, B. A. Stable Isotope Labeling of Phosphoproteins for Large-scale Phosphorylation Rate Determination*. *Molecular & Cellular Proteomics* **2014**, *13* (4), 1106-1118. DOI: https://doi.org/10.1074/mcp.O113.036145.

(36) Yu, K.; Wang, Z.; Wu, Z.; Tan, H.; Mishra, A.; Peng, J. High-Throughput Profiling of ProteomeModificationsProteomesand PosttranslationalModificationsposttranslational Modifications by 16-Plex TMT Labeling and Mass SpectrometryMassspectrometry. In *Quantitative Methods in Proteomics*, Marcus, K., Eisenacher, M., Sitek, B. Eds.; Springer US, 2021; pp 205-224.

(37) Ankney, J. A.; Muneer, A.; Chen, X. Relative and absolute quantitation in mass spectrometry–based proteomics. *Annual review of analytical chemistry* **2018**, *11* (1), 49-77.

(38) Beynon, R. J.; Doherty, M. K.; Pratt, J. M.; Gaskell, S. J. Multiplexed absolute quantification in proteomics using artificial QCAT proteins of concatenated signature peptides. *Nature Methods* **2005**, *2* (8), 587-589. DOI: 10.1038/nmeth774.

(39) Gerber, S. A.; Rush, J.; Stemman, O.; Kirschner, M. W.; Gygi, S. P. Absolute quantification of proteins and phosphoproteins from cell lysates by tandem MS. *Proceedings of the National Academy of Sciences* **2003**, *100* (12), 6940-6945. DOI: 10.1073/pnas.0832254100 (acccessed 2025/03/23).

(40) Kettenbach, A. N.; Rush, J.; Gerber, S. A. Absolute quantification of protein and post-translational modification abundance with stable isotope-labeled synthetic peptides. *Nat Protoc* **2011**, *6* (2), 175-186. DOI: 10.1038/nprot.2010.196 From NLM.

(41) Kito, K.; Ito, T. Mass spectrometry-based approaches toward absolute quantitative proteomics. *Curr Genomics* **2008**, *9* (4), 263-274. DOI: 10.2174/138920208784533647 From NLM.

(42) Ludwig, C.; Claassen, M.; Schmidt, A.; Aebersold, R. Estimation of Absolute Protein Quantities of Unlabeled Samples by Selected Reaction Monitoring Mass Spectrometry *<sup>

</sup>. *Molecular & Cellular Proteomics* **2012**, *11* (3). DOI: 10.1074/mcp.M111.013987 (acccessed 2025/03/23).

(43) Narumi, R.; Shimizu, Y.; Ukai-Tadenuma, M.; Ode, K. L.; Kanda, G. N.; Shinohara, Y.; Sato, A.; Matsumoto, K.; Ueda, H. R. Mass spectrometry-based absolute quantification reveals rhythmic variation of mouse circadian clock proteins. *Proceedings of the National Academy of Sciences* **2016**, *113* (24), E3461-E3467. DOI: 10.1073/pnas.1603799113 (acccessed 2025/03/23).

(44) Nosti, A. J.; Barrio, L. C.; Celis, F. C.; Soldado, A.; Encinar, J. R. Absolute quantification of proteins using element mass spectrometry and generic standards. *Journal of proteomics* **2022**, *256*, 104499.

(45) Raghuraman, B. K.; Bogdanova, A.; Moon, H.; Rzagalinski, I.; Geertsma, E. R.; Hersemann, L.; Shevchenko, A. Median-Based Absolute Quantification of Proteins Using Fully Unlabeled

Generic Internal Standard (FUGIS). *Journal of Proteome Research* **2022**, *21* (1), 132-141. DOI: 10.1021/acs.jproteome.1c00596.

(46) Rzagalinski, I.; Bogdanova, A.; Raghuraman, B. K.; Geertsma, E. R.; Hersemann, L.; Ziemssen, T.; Shevchenko, A. FastCAT Accelerates Absolute Quantification of Proteins Using Multiple Short Nonpurified Chimeric Standards. *Journal of Proteome Research* **2022**, *21* (6), 1408-1417. DOI: 10.1021/acs.jproteome.2c00014.

(47) Schmidt, C.; Urlaub, H. Absolute quantification of proteins using standard peptides and multiple reaction monitoring. *Methods Mol Biol* **2012**, *893*, 249-265. DOI: 10.1007/978-1-61779-885-6_17 From NLM.

(48) Silva, J. C.; Gorenstein, M. V.; Li, G.-Z.; Vissers, J. P. C.; Geromanos, S. J. Absolute Quantification of Proteins by LCMSE: A Virtue of Parallel ms Acquisition *S. *Molecular & Cellular Proteomics* **2006**, *5* (1), 144-156. DOI: https://doi.org/10.1074/mcp.M500230-MCP200.

(49) Yu, K.; Wang, Z.; Wu, Z.; Tan, H.; Mishra, A.; Peng, J. High-Throughput Profiling of Proteome and Posttranslational Modifications by 16-Plex TMT Labeling and Mass Spectrometry. *Methods Mol Biol* **2021**, *2228*, 205-224. DOI: 10.1007/978-1-0716-1024-4_15 From NLM.

(50) Wang, Q.; Liu, Z.; Liu, Y.; Chen, H. Absolute Quantitation of N-Nitrosamines by Coulometric Mass Spectrometry without Using Standards. *J Am Soc Mass Spectrom* **2022**, *33* (5), 875-884. DOI: 10.1021/jasms.2c00064 From NLM.

(51) Xu, C.; Zheng, Q.; Zhao, P.; Paterson, J.; Chen, H. A New Quantification Method Using Electrochemical Mass Spectrometry. *J Am Soc Mass Spectrom* **2019**, *30* (4), 685-693. DOI: 10.1007/s13361-018-2116-6 From NLM.

(52) Zhao, P.; Guo, Y.; Dewald, H. D.; Chen, H. Improvements for absolute quantitation using electrochemical mass spectrometry. *International Journal of Mass Spectrometry* **2019**, *443*, 41-45. DOI: https://doi.org/10.1016/j.ijms.2019.05.017.

(53) Chiu, K.-Y.; Ai, Y.; Tanim-Ai Hassan, M.; Li, X.; Gunawardena, H. P.; Chen, H. Standards-Free Absolute Quantitation of Oxidizable Glycopeptides by Coulometric Mass Spectrometry. *Journal of the American Society for Mass Spectrometry* **2024**, *35* (7), 1441-1450. DOI: 10.1021/jasms.4c00052.

(54) Diehl, G.; Karst, U. On-line electrochemistry – MS and related techniques. *Analytical and Bioanalytical Chemistry* **2002**, *373* (6), 390-398. DOI: 10.1007/s00216-002-1281-3.

(55) Permentier, H. P.; Bruins, A. P.; Bischoff, R. Electrochemistry-mass spectrometry in drug metabolism and protein research. *Mini Rev Med Chem* **2008**, *8* (1), 46-56. DOI: 10.2174/138955708783331586 From NLM.

(56) Li, J.; Dewald, H. D.; Chen, H. Online Coupling of Electrochemical Reactions with Liquid Sample Desorption Electrospray Ionization-Mass Spectrometry. *Analytical Chemistry* **2009**, *81* (23), 9716-9722. DOI: 10.1021/ac901975j.

(57) Chintalapudi, K.; Badu-Tawiah, A. K. An integrated electrocatalytic nESI-MS platform for quantification of fatty acid isomers directly from untreated biofluids. *Chemical Science* **2020**, *11* (36), 9891-9897, 10.1039/D0SC03403G. DOI: 10.1039/D0SC03403G.

(58) Tang, S.; Fan, L.; Cheng, H.; Yan, X. Incorporating Electro-Epoxidation into Electrospray Ionization Mass Spectrometry for Simultaneous Analysis of Negatively and Positively Charged Unsaturated Glycerophospholipids. *J Am Soc Mass Spectrom* **2021**, *32* (9), 2288-2295. DOI: 10.1021/jasms.0c00356 From NLM.

(59) Zhang, X.; Zhan, J.; Yu, Z.; Deng, J.; Li, M.; Shao, Y. Recent Advances in Real-Time Analysis of Electrochemical Reactions by Electrochemical Mass Spectrometry†. *Chinese Journal of Chemistry* **2023**, *41* (2), 214-224. DOI: https://doi.org/10.1002/cjoc.202200523 (acccessed 2025/04/03).

(60) Hu, J.; Zhang, N.; Zhang, P.-K.; Chen, Y.; Xia, X.-H.; Chen, H.-Y.; Xu, J.-J. Coupling a Wireless Bipolar Ultramicroelectrode with Nano-electrospray Ionization Mass Spectrometry: Insights into the Ultrafast Initial Step of Electrochemical Reactions. *Angewandte Chemie International Edition* **2020**, *59* (41), 18244-18248. DOI: https://doi.org/10.1002/anie.202008577 (acccessed 2025/04/03).

(61) Brown, T. A.; Chen, H.; Zare, R. N. Identification of fleeting electrochemical reaction intermediates using desorption electrospray ionization mass spectrometry. *J Am Chem Soc* **2015**, *137* (23), 7274-7277. DOI: 10.1021/jacs.5b03862 From NLM.

(62) Brown, T. A.; Chen, H.; Zare, R. N. Detection of the short-lived radical cation intermediate in the electrooxidation of N,N-dimethylaniline by mass spectrometry. *Angew Chem Int Ed Engl* **2015**, *54* (38), 11183-11185. DOI: 10.1002/anie.201506316 From NLM.

(63) Qiu, R.; Zhang, X.; Luo, H.; Shao, Y. Mass spectrometric snapshots for electrochemical reactions. *Chemical Science* **2016**, *7* (11), 6684-6688, 10.1039/C6SC01978A. DOI: 10.1039/C6SC01978A.

(64) Yu, J.; Zhou, Y.; Hua, X.; Liu, S.; Zhu, Z.; Yu, X.-Y. Capturing the transient species at the electrode–electrolyte interface by in situ dynamic molecular imaging. *Chemical Communications* **2016**, *52* (73), 10952-10955, 10.1039/C6CC02893D. DOI: 10.1039/C6CC02893D.

(65) Wang, Z.; Zhang, Y.; Liu, B.; Wu, K.; Thevuthasan, S.; Baer, D. R.; Zhu, Z.; Yu, X. Y.; Wang, F. In Situ Mass Spectrometric Monitoring of the Dynamic Electrochemical Process at the

Electrode-Electrolyte Interface: a SIMS Approach. *Anal Chem* **2017**, *89* (1), 960-965. DOI: 10.1021/acs.analchem.6b04189 From NLM.

(66) Khanipour, P.; Löffler, M.; Reichert, A. M.; Haase, F. T.; Mayrhofer, K. J. J.; Katsounaros, I. Electrochemical Real-Time Mass Spectrometry (EC-RTMS): Monitoring Electrochemical Reaction Products in Real Time. *Angew Chem Int Ed Engl* **2019**, *58* (22), 7273-7277. DOI: 10.1002/anie.201901923 From NLM.

(67) Hasa, B.; Jouny, M.; Ko, B. H.; Xu, B.; Jiao, F. Flow Electrolyzer Mass Spectrometry with a Gas-Diffusion Electrode Design. *Angewandte Chemie International Edition* **2021**, *60* (6), 3277-3282. DOI: https://doi.org/10.1002/anie.202013713 (acccessed 2025/04/03).

(68) Liu, J.; Yu, K.; Zhang, H.; He, J.; Jiang, J.; Luo, H. Mass spectrometric detection of fleeting neutral intermediates generated in electrochemical reactions. *Chemical Science* **2021**, *12* (27), 9494-9499, 10.1039/D1SC01385H. DOI: 10.1039/D1SC01385H.

(69) Hu, J.; Wang, T.; Zhang, W. J.; Hao, H.; Yu, Q.; Gao, H.; Zhang, N.; Chen, Y.; Xia, X. H.; Chen, H. Y.; et al. Dissecting the Flash Chemistry of Electrogenerated Reactive Intermediates by Microdroplet Fusion Mass Spectrometry. *Angew Chem Int Ed Engl* **2021**, *60* (34), 18494-18498. DOI: 10.1002/anie.202106945 From NLM.

(70) Wan, Q.; Chen, S.; Badu-Tawiah, A. K. An integrated mass spectrometry platform enables picomole-scale real-time electrosynthetic reaction screening and discovery. *Chemical Science* **2018**, *9* (26), 5724-5729, 10.1039/C8SC00251G. DOI: 10.1039/C8SC00251G.

(71) Wang, Q.; Wang, Q.; Zhang, Y.; Mohamed, Y. M.; Pacheco, C.; Zheng, N.; Zare, R. N.; Chen, H. Electrocatalytic redox neutral [3 + 2] annulation of N-cyclopropylanilines and alkenes. *Chemical Science* **2021**, *12* (3), 969-975, 10.1039/D0SC05665K. DOI: 10.1039/D0SC05665K.

(72) Cheng, H.; Yang, T.; Edwards, M.; Tang, S.; Xu, S.; Yan, X. Picomole-Scale Transition Metal Electrocatalysis Screening Platform for Discovery of Mild C-C Coupling and C-H Arylation through in Situ Anodically Generated Cationic Pd. *J Am Chem Soc* **2022**, *144* (3), 1306-1312. DOI: 10.1021/jacs.1c11179 From NLM.

(73) Hsu, C.-C.; Xue, L.; Arrington, J. V.; Wang, P.; Paez Paez, J. S.; Zhou, Y.; Zhu, J.-K.; Tao, W. A. Estimating the Efficiency of Phosphopeptide Identification by Tandem Mass Spectrometry. *Journal of the American Society for Mass Spectrometry* **2017**, *28* (6), 1127-1135. DOI: 10.1007/s13361-017-1603-5.

(74) Ho, H.-P.; Rathod, P.; Louis, M.; Tada, C. K.; Rahaman, S.; Mark, K. J.; Leng, J.; Dana, D.; Kumar, S.; Lichterfeld, M.; et al. Studies on quantitative phosphopeptide analysis by matrix-assisted laser desorption/ionization mass spectrometry without label, chromatography or calibration curves. *Rapid Communications in Mass Spectrometry* **2014**, *28* (24), 2681-2689. DOI: https://doi.org/10.1002/rcm.7063 (acccessed 2025/04/15).

(75) Smith, J. R.; Olivier, M.; Greene, A. S. Relative quantification of peptide phosphorylation in a complex mixture using 18O labeling. *Physiol Genomics* **2007**, *31* (2), 357-363. DOI: 10.1152/physiolgenomics.00096.2007 From NLM.

(76) Yang, N.; Goonatilleke, E.; Park, D.; Song, T.; Fan, G.; Lebrilla, C. B. Quantitation of Site-Specific Glycosylation in Manufactured Recombinant Monoclonal Antibody Drugs. *Analytical Chemistry* **2016**, *88* (14), 7091-7100. DOI: 10.1021/acs.analchem.6b00963.

(77) Huang, Y.; Nie, Y.; Boyes, B.; Orlando, R. Resolving Isomeric Glycopeptide Glycoforms with Hydrophilic Interaction Chromatography (HILIC). *J Biomol Tech* **2016**, *27* (3), 98-104. DOI: 10.7171/jbt.16-2703-003 From NLM.

(78) Lowenthal, M. S.; Liang, Y.; Phinney, K. W.; Stein, S. E. Quantitative bottom-up proteomics depends on digestion conditions. *Anal Chem* **2014**, *86* (1), 551-558. DOI: 10.1021/ac4027274 From NLM.

(79) Zhao, J.; Peng, W.; Dong, X.; Mechref, Y. Analysis of NIST Monoclonal Antibody Reference Material Glycosylation Using the LC-MS/MS-Based Glycoproteomic Approach. *J Proteome Res* **2021**, *20* (1), 818-830. DOI: 10.1021/acs.jproteome.0c00659 From NLM.
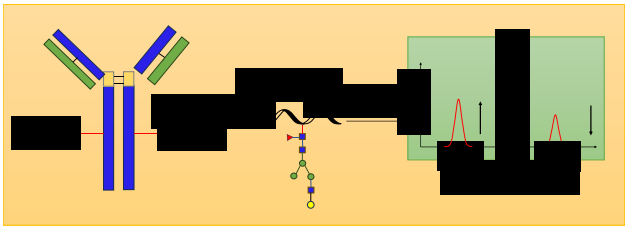
Graphic abstract